

THE GREAT ANNIHILATOR 1E1740.7-2942: MOLECULAR CLOUD CONNECTION AND CORONAL STRUCTURE.

Osmi Vilhu, Diana Hannikainen, Panu Muhli and Juhani Huovelin

Observatory, University of Helsinki, Finland

Juri Poutanen

Stockholm Observatory, Saltsjöbaden, Sweden

Philippe Durouchoux

DAPNIA, Service d'Astrophysique, CE Saclay, France

Pierre Wallyn

Jet Propulsion Laboratory, CalTech, USA

ABSTRACT

Using ^{12}CO and ^{13}CO observations we present column density maps of the molecular cloud ($V_{LSR} = -135 \text{ km/s}$) in the direction of 1E1740.7-2942. Hydrogen column densities of the cloud scatter between $N_H = (3.5 - 11) \times 10^{22} \text{ cm}^{-2}$, depending on the method used. From this we conclude, deriving first a simple analytic formula, that despite of the weakness of the iron fluorescent 6.4 keV line (Churazov et al. 1996) the source may lie inside the cloud, or at least close to its edge. The combined ASCA/BATSE spectrum from September 1993 and 1994 can be modelled with a two-phase accretion disc corona model, where the hot region is detached from the cold disc. Geometrically the hot phase can be interpreted e.g. as a number of active regions (magnetic loops) above the disc, or as a spherical hot cloud around the central object.

Keywords: Galactic Center, Black hole candidates, Molecular clouds, Gamma-ray spectra, accretion discs

1. INTRODUCTION

The discovery of a massive molecular cloud (at $V_{LSR} \approx -130 \text{ km/s}$) in the direction of the bright X-ray source 1E1740.7-2942 (Bally and Leventhal 1991; Mirabel et al. 1991) raised a picture of a compact source embedded in a molecular cloud. It was suggested that the unique properties of this object are related to the presence of dense gas surrounding it. In particular, the Bondi-Hoyle accretion onto a single black hole was discussed.

The ASCA data imply $N_H = 8 \times 10^{22} \text{ cm}^{-2}$ for the

low energy absorption (Sheth et al. 1996), and twice of that for the iron K-edge absorption (Churazov et al. 1996). Based on these column density estimates Churazov et al. concluded that the weakness of the iron 6.4 keV line suggests that the source is located behind the cloud.

2. THE MOLECULAR LINE OBSERVATIONS

The observations were performed between August 1 - 8, 1993, using the Swedish ESO Submillimeter Telescope (SEST) situated at La Silla in Chile. The front-end was a Schottky receiver and the 1086 MHz bandwidth acousto-optical spectrometer (AOS) was used as the back-end. The intensity calibration was performed using the chopper-wheel method, the background was eliminated with the position switching mode. The half power beamwidth (FWHM) of the telescope at 115 GHz is 45 arc sec.

We observed two lines $^{12}\text{CO}(J=1-0)$ (115 GHz) and $^{13}\text{CO}(J=1-0)$ (110 GHz) at 35 spatial positions around 1E1740.7-2942. In both transitions the line at $V_{LSR} = -135 \text{ km/s}$ can be clearly identified (Fig. 1) and the antenna brightness temperature was integrated between -115 km/s and -150 km/s to give the total flux F_{cloud} . Three different methods were used to calculate $N_H = 2 \times N(\text{H}_2)$:

Method 1. The standard conversion (see Bally and Leventhal 1991; Fig. 2)

$$N(\text{H}_2)/F_{\text{cloud}}(^{12}\text{CO}) = 2.6 \times 10^{20} \text{ cm}^{-2}/\text{K km s}^{-1}.$$

Method 2. Scaling with the LTE-relation given by Bally and Leventhal (1991) with $T_{exc} = 15 \text{ K}$ (see Fig. 3)

$$N(H_2)/F_{\text{cloud}}(^{13}\text{CO}) = 5.1 \times 10^{20} \text{ cm}^{-2}/\text{K km s}^{-1}.$$

Method 3. Assuming LTE like in the method 2, but computing T_{exc} and τ with the help of ^{12}CO and ^{13}CO , and finally using the conversion $N(H_2) = 1.0 \times 10^6 \times N(^{13}\text{CO})$ (Gahm et al. 1993; see Fig. 4).

The column density maps based on these methods are shown in Figures 2-4. In the direction of 1E1740.7-2942, the methods 1, 2 and 3 give values of $N_H = 11$, 3.5 and 7, respectively (in units of 10^{22} cm^{-2} and in the position of the circle centrum in Figs. 2 - 4).

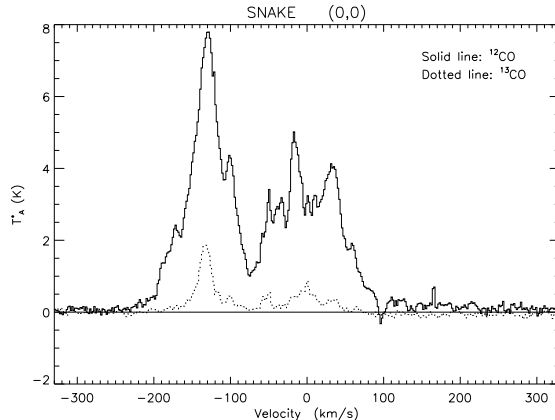


Figure 1: ^{12}CO (solid) and ^{13}CO (dotted) spectra at the $(0,0)$ position of the maps in Figs. 2-4.

3. IS 1E1740.7-2942 INSIDE THE CLOUD?

Churazov, Gilfanov and Sunyaev (1996) showed that in the ASCA data there is no (or very weak) evidence of the fluorescent iron line at 6.4 keV. The line equivalent width is smaller than 20 eV with 90 per cent confidence, the 'best value' being around 10 eV. Further, Churazov et al. showed that the column must be less than $(2 - 3) \times 10^{22} \text{ cm}^{-2}$, if the source is in the center of the cloud. They concluded that 1E1740.7-2942 is behind the cloud.

Our measurements in the direction of 1E1740.7-2942 $N_H = (3.5 - 11) \times 10^{22} \text{ cm}^{-2}$ suggest that the source location may be behind the cloud to explain both the iron K-edge absorption and the standard IS-absorption in this general direction $(5 - 7) \times 10^{22} \text{ cm}^{-2}$ (Sheth et al. 1996). However, since the total column (integrating over all velocities in Fig. 1) is large ($6 \times 10^{23} \text{ cm}^{-2}$), 1E1740.7-2942 may equally well lie in front of the cloud.

Assume that 1E1740.7-2942 is at a distance d from the centre of a spherical homogeneous cloud with radius r . For a Thomson optically thin cloud, it is rather simple algebra to derive the following relation between the equivalent width EW of the fluorescent line, $a \equiv d/r$, the column density across the cloud center N_H and iron abundance N_{Fe} (number den-

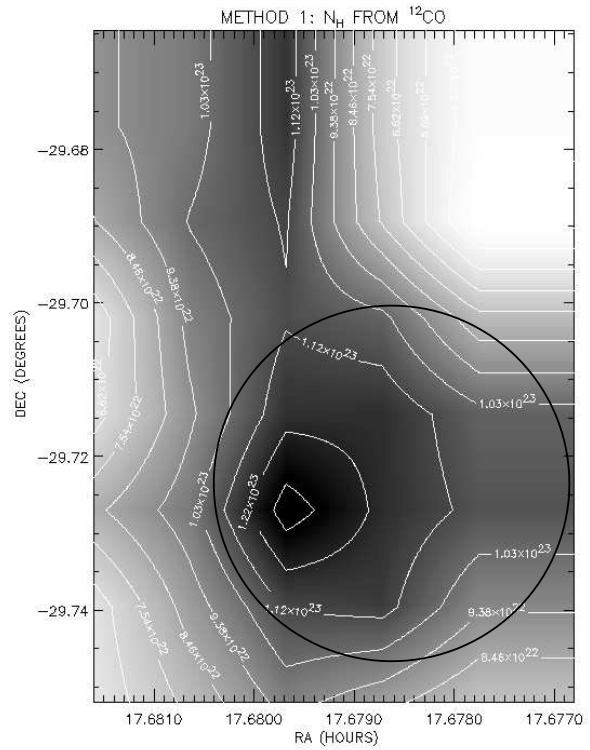


Figure 2: The Hydrogen column density map around 1E1740.7-2942 from the ^{12}CO line observations with a linear scaling (method 1, see the text). The ASCA resolution circle (PSF diameter 2.9 arc min = 7 pc at 8.5 kpc) centered at the radio-jets (Mirabel et al. 1992) is shown. The darkest region corresponds to the largest column density. The range of N_H is between $(9 - 13) \times 10^{22} \text{ cm}^{-2}$ inside the circle.

sity):

$$\text{EW} = 30 N_{H,23} (N_{\text{Fe}}/N_{\text{Fe}\odot}) G(a), \quad (1)$$

where the equivalent width EW is in units of eV, column density is in units of 10^{23} cm^{-2} , and the geometrical factor $G(a)$ is given by the formula:

$$G(a) = \frac{1}{2} \left[1 + \frac{1-a^2}{2a} \ln \frac{1+a}{|1-a|} \right]. \quad (2)$$

To derive the numerical factor in equation 1 we used the same values for the absorption cross section at the iron K-edge ($3.5 \times 10^{-20} \text{ cm}^2$ per iron atom) and for the fluorescent yield ($W = 0.35$) as Churazov et al. (1996) did.

For a solar abundance of iron ($N_{\text{Fe}}/\text{NH} = 10^{-4.5}$), this equation predicts $a = 1.1$ (i.e. the source is close to the edge of the cloud) for the largest column $N_H = 11 \times 10^{22} \text{ cm}^{-2}$ (method 1) and for the 'best' $\text{EW} = 10$ eV derived by Churazov et al.. The smallest column from the method 2 (3.5×10^{22}) gives $a = 0.1$ (i.e. the source is close to the center of the cloud). Values of a range between 0.9 and 1.5 for $N_{\text{Fe}} = 2N_{\text{Fe}\odot}$ which can not be rejected due to the large observed iron K-edge.

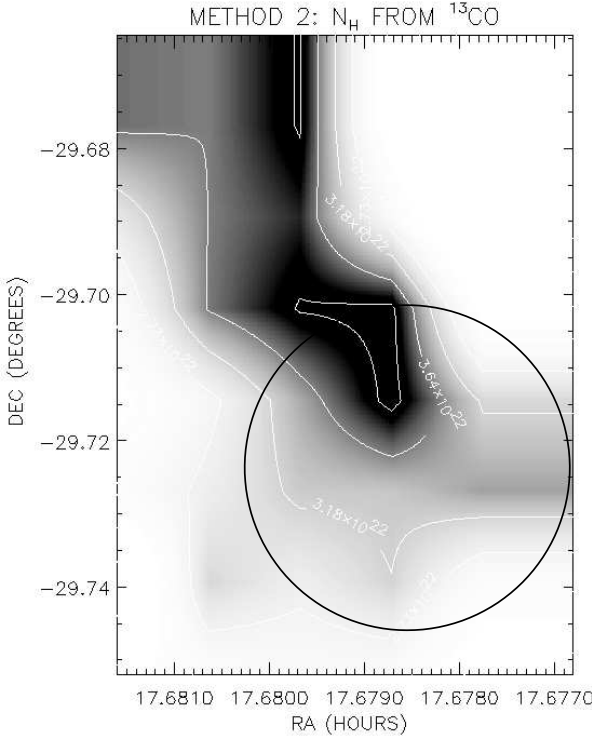


Figure 3: As in Fig. 2, but from the ^{13}CO line observations with a linear scaling (method 2, see the text). The darkest regions correspond to the largest column density. The range of N_{H} is between $(3 - 4) \times 10^{22} \text{ cm}^{-2}$ inside the circle.

The real column of the cloud might be somewhat different from the values used. However, the size of the scattering induced area inside the ASCA resolution circle is small enough to make our estimates reasonably good (see Figs. 2 - 4, extreme values of N_{H} range between $(3 - 13) \times 10^{22} \text{ cm}^{-2}$ inside the circles). After all, the largest uncertainties in column density estimates come from the method used.

4. ASCA/BATSE SPECTRAL MODELLING

We attempted spectral modelling using two-phase disc-corona models described by Poutanen and Svensson (1996). In these models, soft radiation from the accretion disc gets comptonized by hot electron (-positron) gas in the corona. Different coronal geometries can be considered: slab, hemisphere, and cylinder. The effects of different viewing angles and separation of the hot active regions from the disc (covering factor g) can also be modelled. This is particularly relevant to 1E1740.7-2942, since the weakness of the iron line suggests that the reflection component is small. This means that the disc is viewed edge-on and/or the cold disc covers much less than 2π solid angle as viewed from the X-ray source.

The models with large g tend to have too small fluxes at BATSE energies. To compensate this one can decrease the number of reprocessed soft photons enter-

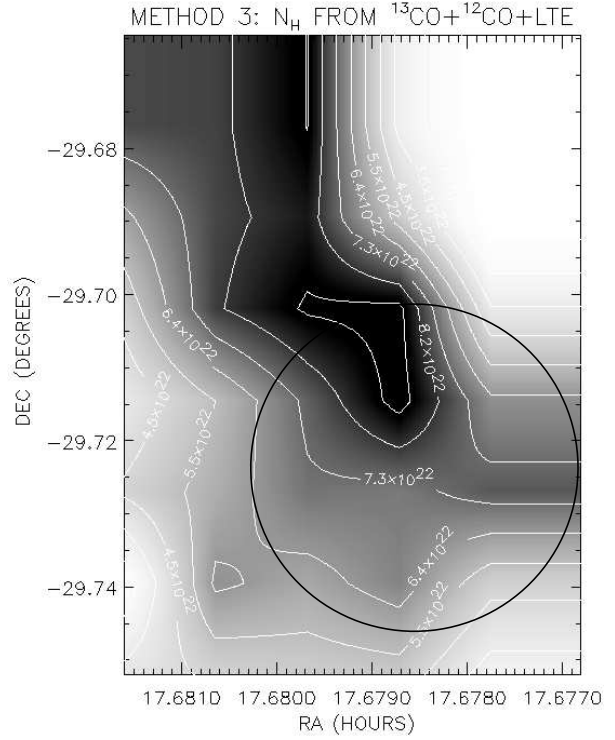


Figure 4: As in Figs. 2 and 3, but from the LTE method using ^{12}CO and ^{13}CO (method 3, see the text). The darkest regions correspond to the largest column density. The range of N_{H} is between $(5 - 9) \times 10^{22} \text{ cm}^{-2}$ inside the circle.

ing the corona (small g -factor). By the energy balance this increases the optical depth, allowing more scattering orders at BATSE energies. Geometrically small g means that the hot corona is **detached from the disc** (like apexes of **magnetic coronal loops**) or is **situated in a central hole** inside the classical disc (Shapiro et al. 1976, Narayan 1996).

We used as input observations those from ASCA (Sheth et al. 1996) and from the simultaneous BATSE archive observations analyzed by the JPL earth occultation method (Wallyn et al. 1996). We do not attempt to give 'the best fit' model, just demonstrate one possible model.

Figure 5 shows the average ASCA spectrum (September 26, 1993 and September 9-12, 1994; Sheth et al. 1996) fitted well with a power-law fit ($\alpha = 1.1$ and $N_{\text{H}} = 8 \times 10^{22} \text{ cm}^{-2}$), together with the BATSE data averaged over 13 days around the ASCA observing dates. In addition, the BATSE standard state spectrum is shown (high state minus low state in the 1989 - 91 data to subtract the apparent background contamination). The spectrum obtained in this way is almost identical to the SIGMA standard state spectrum (Sunyaev et al. 1991). The high energy rise can not be modelled with thermal models. It needs a separate physical component, and part of that may come from a possible diffuse radiation in the BATSE field of view.

Models with hemisphere type active regions are over-

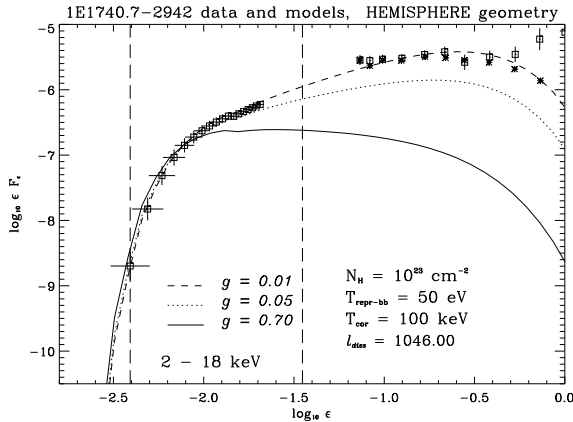


Figure 5: The average ASCA spectrum of 1E1740.7-2942 from September 26, 1993, and September 9-12, 1994 (Sheth et al. 1996), together with the BATSE spectrum averaged over 13 days around these dates (data points with error bars). The standard state BATSE spectrum (almost identical to the standard SIGMA spectrum by Sunyaev et al. 1991) is also shown (stars). Edge-on models with no reflection component and with detached active regions are overplotted ($g = 0.05$ and 0.01). For comparison, the same model with active regions in touch with the disc is shown by the solid line ($g = 0.7$). The x -axis is $\log_{10}\epsilon$ where $\epsilon = E(\text{keV})/511$ and the y -axis equals to $\log_{10}(\epsilon^2 F_{ph})$ where F_{ph} is the observed photon flux ($\text{ph}/\text{cm}^2/\text{sec}/\text{keV}$).

plotted in Figure 5. They have coronal temperature $T_{cor} = 100$ keV and soft photons black body temperature $T_{bb} = 50$ eV. The models are edge-on and the reflection component was switched off due to the weakness of the iron line. Different geometrical factors were used (e.g. $g = 0.01$ corresponds to the case when 1% of the radiation reprocessed and reflected from the cold disc enters back the active region). The optical depths for the models with $g = 0.7, 0.05$ and 0.01 are 1.05, 2.8 and 3.75, respectively.

In the case of electron-positron pair dominated corona, the compactness parameter $l_{diss} = (L/H)(\sigma_T/m_e c^3)$ can be used to estimate the dimension H of the active region. Assuming the luminosity $L = 3 \times 10^{37}$ ergs/s for the standard state (Sunyaev et al. 1991), one obtains for the best model in Fig. 5 with $g = 0.01$ ($l_{diss} = 1046$) $H = 8 \times 10^5$ cm. This corresponds to $3R_{Sch}$ for a solar mass central object. This type of central hot flow solutions were found already by Shapiro et al. (1976). For hotter T_{cor} this dimension increases to match better with a more massive BH. Assuming many active regions, H scales inversely with the number. For e^+e^- -pairs in the active region, the number density can be estimated in the model as $n = 1.5 \times 10^{24}\tau/H \approx 7 \times 10^{18}\text{cm}^{-3}$.

Gahm, G. F., Johansson, L. E. B., Liseau, R. 1993, A&A, 274, 415
 Mirabel, I. F., et al. 1991, A&A, 251, L43
 Mirabel, I. F., Rodriguez, L. F., Cordier, B., Paul, J., Lebrun, F. 1992, Nature, 358, 215
 Narayan, R. 1996, ApJ, 462, 136
 Poutanen, J., Svensson, R. 1996, ApJ, 470, 249.
 Shapiro S.L., Lightman A.P., Eardley D.M. 1976, ApJ, 204, 187.
 Sheth, S., Liang, E., Luo, C. 1996 (preprint)
 Sunyaev, R., et al. 1991, ApJ, 383, L49
 Wallyn, P., Ling, J. C., Wheaton, Wm. A., Mahoney, W. A., Radocinski, R. G., Skelton, R. T. 1996, ApJ (in press)

REFERENCES

Bally, J., Leventhal, M. 1991, Nature, 353, 234
 Churazov, E., Gilfanov, M., Sunyaev, R. 1996, ApJ, 470, L71.